

# Adaptive pulse compression for transform-limited 15-fs high-energy pulse generation

E. Zeek, R. Bartels, M. M. Murnane, H. C. Kapteyn, and S. Backus

*JILA, University of Colorado at Boulder, Boulder, Colorado 80309-0440*

G. Vdovin

*Electronic Instrumentation, Delft University of Technology, 2600 GA Delft, The Netherlands*

Received November 23, 1999

We demonstrate the use of a deformable-mirror pulse shaper, combined with an evolutionary optimization algorithm, to correct high-order residual phase aberrations in a 1-mJ, 1-kHz, 15-fs laser amplifier. Frequency-resolved optical gating measurements reveal that the output pulse duration of 15.2 fs is within our measurement error of the theoretical transform limit. This technique significantly reduces the pulse duration and the temporal prepulse energy of the pulse while increasing the peak intensity by 26%. It is demonstrated, for what is believed to be the first time, that the problem of pedestals in laser amplifiers can be addressed by spectral-domain correction. © 2000 Optical Society of America

*OCS codes:* 140.7090, 140.3590, 320.5540, 320.5520.

The past five years have seen considerable improvements in the capabilities of high-power ultrafast lasers. Ti:sapphire-based oscillator–amplifier systems can generate peak powers of  $\sim 100$  TW at 10 Hz, or 0.3–1 TW at kilohertz repetition rates.<sup>1–3</sup> The pulse duration that is obtainable from these systems has also decreased from  $\sim 100$  to  $\sim 20$  fs. However, at very short pulse durations ( $< 20$  fs), pulses from these systems often suffer from poor peak-to-background contrast in the time domain. This poor contrast results from imperfect correction of the spectral phase arising from large amounts of refractive material in the laser amplifier system, because compensating for this material requires that the pulse compressor be mismatched from the stretcher. Imperfect optics and alignment can also contribute to residual dispersion. This results in energy arriving before and (or) after the peak of the pulse, and this prepulse reduces the utility of the laser pulses for many experiments, such as ultrafast x-ray generation,<sup>4,5</sup> attosecond pulse generation, and ultrafast laser plasmas,<sup>6</sup> including solid-target high-harmonic generation<sup>7</sup> and novel absorption mechanisms.<sup>8</sup> Researchers have employed various schemes incorporating prisms, complex stretcher–compressor designs, and ultrahigh-precision optics to compensate for up to the fourth-order phase in a Taylor expansion.<sup>2,9,10,11</sup> However, very complex phase aberrations can arise from the use of chirped mirrors<sup>12</sup> and intracavity etalons<sup>13</sup> in an amplifier system; to date, these aberrations have been impossible to compensate for completely. Recently, pulse shapers with liquid crystals<sup>14</sup> have been used to adaptively correct<sup>15</sup> for amplifier-induced spectral phase distortions.<sup>16–18</sup> However, in this past work, substantially improved laser-pulse characteristics over what could be obtained by use of conventional means were not demonstrated.

Here we present a versatile, low-cost spectral phase correction technique that uses a deformable-mirror pulse shaper.<sup>19</sup> This device allows the efficient removal of high-order phase distortions automati-

cally and without introducing additional aberrations, allowing us to generate 15-fs, 1-mJ pulses from a kilohertz laser amplifier system that are transform limited. The pulses were characterized by use of second-harmonic frequency-resolved optical gating,<sup>20</sup> with a dynamic range of  $10^{-4}$ . This technique is of great importance to a variety of high-field science experiments that are sensitive to prepulse. This approach has a very substantial advantage over previous time-domain techniques<sup>21</sup> in that it corrects for, rather than filters out, pulse aberrations. Thus the peak intensity of the contrast-enhanced pulses is higher, rather than lower, after correction. This higher intensity allows us to generate high-energy pulses that are significantly shorter than previously demonstrated and allows for a new level of precision in the study of high-field laser–matter interactions by use of light pulses that are only a few optical cycles in duration.

The laser amplifier system used in this work is similar to that described previously,<sup>2</sup> with two changes (see Fig. 1). First, the conventional lamp-pump frequency-doubled Nd:YAG pump laser is replaced with a diode-pumped laser. Second, a pulse shaper<sup>19</sup> is inserted into the beam just after the pulse stretcher. Pulses are first injected into an all-reflective stretcher before entering the pulse shaper, which consists of a 4-*f* zero-dispersion stretcher employing a micromachined deformable mirror (MMDM) at the fold plane. A 600-mm radius-of-curvature mirror is used in the pulse shaper, resulting in a spot size of 170- $\mu\text{m}$  diameter for

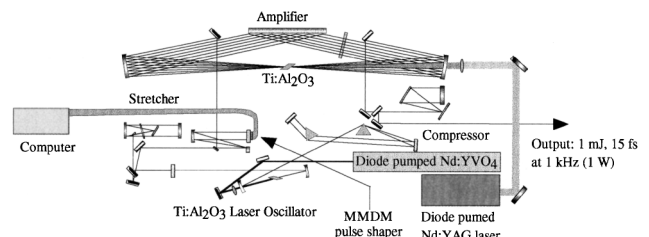


Fig. 1. 15-fs amplifier system with a MMDM pulse shaper.

a discrete color at the focal plane where the MMDM is located. The 318-g/mm grating in the pulse shaper results in a spectral aperture of  $\sim 200$  nm, mapped onto the 30-mm width of the MMDM. The average fluence on the mirror is  $\sim 3$  W/cm<sup>2</sup>, well below the damage threshold of the mirror. The mirror itself is a 600 nm thick  $\times 30$  mm  $\times 10$  mm silicon nitride membrane coated with gold. After it is coated, the membrane is suspended over a linear array of 19 electrodes, which forms the controlling structure of the membrane. A voltage applied to an electrode attracts the membrane, distorting the surface.

High-repetition-rate kilohertz amplifiers are typically pumped by arc-lamp-pumped Nd:YLF lasers, with pulse durations of  $\sim 160$  ns. In high-gain amplifier systems such as the one used in this work (single-pass gain,  $\sim 8\times$ ), significant amplified spontaneous emission can build up during the pump pulse, depleting the gain. In this work we use an intracavity-doubled diode-pumped Nd:YAG laser (Cutting Edge Optronics) that delivers 50-ns pulses. The shorter pump pulse allows for higher gain in the Ti:sapphire amplifier before amplified spontaneous emission buildup, increasing the overall amplifier efficiency and bandwidth. The pulses injected into the amplifier have a 125-nm FWHM bandwidth, which narrows to 84 nm after amplification to 1.4-mJ energy for 8-W pump power. The optical efficiency of 17.5% compares well with the previously obtained value of 9.2%,<sup>22</sup> with a wall-plug efficiency of  $\sim 0.14\%$ . After they are amplified, the pulses are recompressed by use of a standard two-grating (1200-g/mm) compressor.<sup>22</sup>

Typical output without the adaptive pulse shaper is an 18–20-fs pulse with 1 mJ of energy. Figure 2 shows second-harmonic frequency-resolved optical gating measurements<sup>20</sup> of [curve (a)] the pulse spectral intensity and [curve (b)] group delay. Since the MMDM can compensate only for a limited amount of phase aberration (corresponding to dispersion of approximately 12 mm of material<sup>19</sup>), it is necessary to model the system and adjust it to near optimum before applying the MMDM compensation. In Fig. 2, curves (c) and (d) show the pulse spectrum and the group delay, respectively, predicted by a numerical model of the pulse amplifier system.<sup>2</sup> The agreement with curves (a) and (b) is excellent.

An evolutionary strategy (ES) feedback algorithm was employed to determine the optimum settings of the MMDM.<sup>23</sup> The feedback signal into the ES algorithm was the intensity of the second-harmonic-generation frequency-resolved optical gating signal set at zero time delay. The algorithm increased the total intensity of this signal. The advantage of this type of optimization is that it requires no calibration of the apparatus and is very fast. Even after running the optimization algorithm for only  $\sim 5$  min, we find that the group delay is much improved, as shown by curve (e) of Fig. 2, varying  $<15$  fs from peak to valley over the entire spectrum. Figure 3 shows the pulse output in the time domain. As shown in Fig. 3, before optimization the pulse FWHM is 18 fs, whereas after optimization it is 15.2 fs—within our measurement error of  $\pm 0.1$  fs of the transform-limited

value of 15.1 fs. The pulse contrast (i.e., the peak-to-peak intensity ratio) is also improved from the best case before optimization. The pulse intensity  $\sim 25$  fs from the peak of the pulse is suppressed by more than an order of magnitude. The resulting measured pulse shape is near the transform limit down to the noise floor of our measurements ( $\sim 10^{-4}$ ). The pulse's peak intensity also improves by 26% as a result of optimization.

The ES algorithm is a powerful technique for general optimization. It is similar to genetic algorithms, in that it uses evolution as a model for optimization. The ES relies on random mutation of the best solutions from the previous generation to sample new areas in parameter space. We use an adaptive mutation strategy to control the generation of new trials. Part of the genetic code for each trial is a mutation-rate variable. Initial trials are generated randomly. New trials are generated by addition of a normally distributed random variable, with a distribution width characterized by the mutation rate, to the parents, which includes the mutation-rate variable itself. From a set of 20 parent trails, 100 children are generated in each iteration. As the algorithm settles on an optimum solution, solutions with a lower mutation rate naturally become more

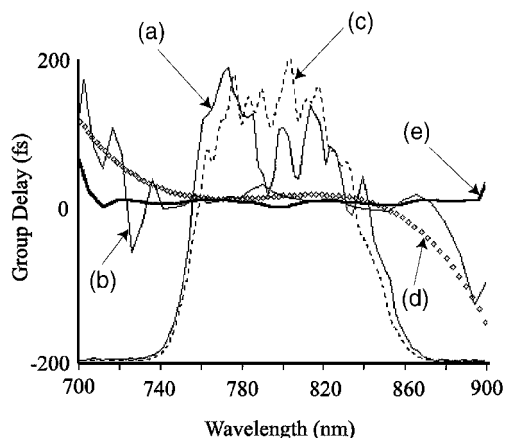


Fig. 2. Amplifier output: (a) pulse spectrum before optimization, (b) group delay before optimization, (c) predicted spectrum before optimization, (d) predicted group delay before optimization, (e) measured group delay after optimization.

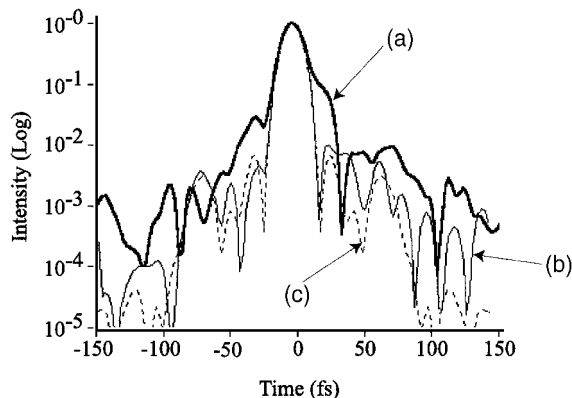


Fig. 3. Output pulse on a logarithmic scale: (a) before optimization (18 fs), (b) after optimization (15.2 fs), (c) transform limit of the measured spectrum (15.1 fs).

robust. The response time of the MMDM is in the millisecond range, making a search practical. In our system, optimization takes approximately 5–10 min, limited by the speed of the software. The millisecond response time of the mirror will allow for further improvements, although it may be limited by pulse-to-pulse fluctuations in the case of 1-kHz repetition-rate amplifiers.

This work clearly demonstrates that feedback by use of second-harmonic generation is extraordinarily effective in optimizing pulse characteristics, even in a laser amplifier in which the pulse-to-pulse fluctuations are quite substantial, approximately 3% in the laser used here. Yet the second-harmonic-generation feedback demonstrably improves pulse characteristics even in the wings, where the intensity is  $\sim 10^{-4}$  of the peak intensity. This improvement results from the fact that the MMDM serves to redistribute the frequency components of the pulse, rather than simply filtering out undesired components. A numerical integration of the temporal profiles of Fig. 3 (assuming no change in total pulse energy, as is the case) shows that the optimization increased the peak intensity by 26% over the unoptimized value, to within 6% of the transform limit. This 26% increase results from the fact that the MMDM optimization transfers energy that was originally spread over hundreds of femtoseconds to the peak of the pulse.

We note that previous work on optimization of amplifier systems was done with liquid-crystal (LC) modulators. Efimov and Reitze demonstrated correction of high-order dispersion to reduce pulse duration in a millijoule multipass amplifier from 32 to 26 fs (Ref. 17); Brixner *et al.* demonstrated compression of pulses from 195 to 103 fs.<sup>18</sup> In previous work adaptive compression of low-energy pulses by use of a LC was also demonstrated.<sup>15</sup> There are distinct advantages and disadvantages to LC and MMDM systems. The LC modulates the light in discrete spectral intervals because of the pixelated nature of the device, resulting in the generation of pulse artifacts that will limit the pulse contrast that can be achieved.<sup>14,15</sup> The MMDM provides smooth modulation with no artifacts. However, the MMDM cannot easily provide amplitude modulation, whereas the LC can. The LC also has a greater number of actuators, increasing its versatility for correcting complex phase aberrations. This increased versatility also increases the number of adjustable parameters, making it in principle slower and more difficult for the evolutionary algorithm to optimize compression. To our knowledge no past work in adaptive pulse compression examined the resulting pulses with high dynamic range. Therefore it is quite possible that after LC optimization a few frequency components remained unoptimized and created a pulse pedestal. The results presented here are a significant improvement over what has been accomplished with LC technology, at significantly lower cost.

In summary, we have demonstrated are the highest-contrast sub-20-fs high-energy laser pulses yet generated and the shortest pulses yet obtained from such a system. Significant improvements in pulse intensity,

pulse quality, and prepulse reduction were obtained as a result of optimization.

We gratefully acknowledge support for this research from the U.S. Department of Energy and the National Science Foundation. S. Backus's e-mail address is sbackus@jila.colorado.edu.

## References

1. V. Bagnoud and F. Salin, in *Digest of Conference on Lasers and Electro-Optics*, 1999 OSA Technical Digest Series (Optical Society of America, Washington, D.C., 1999), p. 71–72.
2. S. Backus, C. Durfee, M. M. Murnane, and H. C. Kapteyn, *Rev. Sci. Instrum.* **69**, 1207 (1998).
3. K. Yamakawa, M. Aoyama, S. Matsuoka, T. Kase, Y. Akahane, and H. Takuma, *Opt. Lett.* **23**, 1468 (1998).
4. R. W. Schoenlein, W. P. Leemans, A. H. Chin, P. Wolfbeyn, T. E. Glover, P. Balling, M. Zolotorev, K. J. Kim, S. Chattopadhyay, and C. V. Shank, *Science* **274**, 236 (1996).
5. A. Rundquist, C. G. Durfee III, S. Backus, C. Herne, Z. Chang, M. M. Murnane, and H. C. Kapteyn, *Science* **280**, 1412 (1998).
6. C. W. Siders, S. P. LeBlanc, D. Fisher, T. Tajima, M. C. Downer, A. Babine, A. Stepanov, and A. Sergeev, *Phys. Rev. Lett.* **76**, 3570 (1996).
7. D. Linde, *Appl. Phys. B* **68**, 315 (1999).
8. M. K. Grimes, A. R. Rundquist, Y.-S. Lee, and M. C. Downer, *Phys. Rev. Lett.* **82**, 4010 (1999).
9. B. E. Lemoff and C. P. J. Barty, *Opt. Lett.* **18**, 1651 (1993).
10. V. Bagnoud and F. Salin, *J. Opt. Soc. Am. B* **16**, 188 (1999).
11. D. Fittinghoff, B. Walker, J. Squier, C. Toth, C. Rose-Petruck, and C. Barty, *IEEE J. Sel. Top. Quantum Electron.* **4**, 430 (1998).
12. R. Szipocs, K. Ferencz, C. Spielman, and F. Krausz, *Opt. Lett.* **19**, 201 (1994).
13. C. Barty, G. Korn, F. Raksi, C. Rose-Petruck, J. Squier, A. Tian, K. Wilson, V. Yakovlev, and K. Yamakawa, *Opt. Lett.* **21**, 219 (1996).
14. M. Wefers and K. Nelson, *J. Opt. Soc. Am. B* **12**, 1343 (1995).
15. D. Yelin, D. Meshulach, and Y. Silberberg, *Opt. Lett.* **22**, 1793 (1997).
16. A. Efimov, M. Moores, N. Beach, J. Krause, and D. Reitze, *Opt. Lett.* **23**, 1915 (1998).
17. A. Efimov and D. Reitze, *Opt. Lett.* **23**, 1612 (1998).
18. T. Brixner, M. Strehle, and G. Gerber, *Appl. Phys. B* **68**, 281 (1999).
19. E. Zeek, K. Maginnis, S. Backus, U. Russek, M. Murnane, G. R. Mourou, H. Kapteyn, and G. Vdovin, *Opt. Lett.* **24**, 493 (1999).
20. R. Trebino, K. DeLong, D. Fittinghoff, J. Sweetser, M. Krumbugel, B. Richman, and D. Kane, *Rev. Sci. Instrum.* **68**, 3277 (1997).
21. S. Backus, H. C. Kapteyn, M. M. Murnane, D. M. Gold, H. Nathel, and W. White, *Opt. Lett.* **18**, 134 (1993).
22. S. Backus, C. G. I. Durfee, G. A. Mourou, H. C. Kapteyn, and M. M. Murnane, *Opt. Lett.* **22**, 1256 (1997).
23. J. Heitkotter and D. Beasley, "The hitchhiker's guide to evolutionary computation (FAQ)," USENET: comp.ai.genetic (1997).